## 15.1 Large-Scale Acquisition of Large-Area Sensors Using an Array of Frequency-Hopping ZnO Thin-Film-Transistor Oscillators

Yasmin Afsar, Tiffany Moy, Nicholas Brady, Sigurd Wagner, James C. Sturm, Naveen Verma

Princeton University, Princeton, NJ

Hybrid systems combine Large-Area Electronics (LAE) and silicon CMOS ICs for sensing and computation, respectively. Such systems are limited in number of sensors by the interfaces required between LAE and CMOS. One solution is active matrices; however, these are best suited to highly-regular sensor arrangements due to many speed/power-limiting data lines, and ultimately provide only a square-root reduction in the number of interfaces. This paper presents a large-area pressure-sensing system that achieves a much greater reduction in the number of interfaces from distributed LAE sensors to CMOS via an array of frequency-hopping, injection-locked, ZnO-TFT digitally-controlled oscillators (DCOs).

Figure 15.1.1 shows the system architecture. Each of the M LAE sensors has its own DCO, and all DCOs (via capacitors $C_C$) combine into a single differential signal, held at virtual ground in the CMOS domain for current sensing. The sensors modulate the DCO amplitudes, and a digital hopping code H[N-1:0] from CMOS modulates the DCO frequencies to one of $2^N$ channels. The H[N-1:0] hopping-code bits are hardwired differently to the frequency-control bits X[N-1:0] of each DCO. In this way, scanning across all H[N-1:0] hopping-code values yields a unique frequency-hopping sequence for each DCO, allowing a large number of sensors to be accessed. This gives combinatorial scaling that enables many more sensors than active-matrix (or even binary) addressing (Fig. 15.1.1) for a fixed number of interfaces between the sensors and the CMOS ICs. The prototype demonstrates 8 frequency channels (N = 3) and 18 sensors.

Figure 15.1.2 shows each DCO, consisting of a cross-coupled pair of TFTs and an LC tank (capacitance set by TFT parasitics) for oscillation, a tail TFT for amplitude modulation via sensor signals $V_{S,i}$, and banks of switched, binary-weighted capacitors $C_{B,b}$, for frequency modulation via X[N-1:0]. While most LAE topologies are limited by low TFT $f_T$ ( ~ 10MHz), LC oscillators exploit high-Q planar inductors possible in LAE (physically large inductors with wide traces and many turns) to resonate with the TFT capacitances. This enables oscillators limited instead by $f_{MAX}$, which can be made higher than $f_T$ in TFTs by reducing the gate resistance [1]. Figure 15.1.2 shows the measured TFT $f_T$ (H21 = 0dB), $f_{MAX}$ (MAG = 0dB), and oscillator output with frequency near $f_{MAX}$. High-frequency, high-Q oscillations enable the large number of frequency channels needed for the combinatorial scaling in Fig. 15.1.1. The DCO amplitude $V_{DCO,i}$ is set by sensor signal $V_{S,i}$ at the tail TFT, with source degeneration (Fig. 15.1.2) enhancing linearity of the $V_{S,i}$-to-$V_{DCO,i}$ transfer function. Hopping between frequency channels requires a TFT switch for each $C_{B,b}$. Each TFT switch is proportionately widened to give a small deep-triode on-resistance $R_{ON,b}$, such that the time constant $R_{ON,b}C_{B,b}$ is much faster than the highest frequency channel, while its capacitance $C_{GD,b}$ is kept much smaller than $C_{B,b}$. This tradeoff allows high channel frequencies ( ~ 15MHz). For the prototype, a conservative design point is chosen with $C_{B,0}$ = 15pF, giving nominal channel frequencies $f_0 \ldots f_7$: 1.36 / 1.27 / 1.20 / 1.13 / 1.07 / 1.03 / 0.99 / 0.95 MHz.

Figure 15.1.3 shows the fast frequency-hopping scheme (i.e. $V_{S,i}$ constant throughout the H[2:0] sequence). Each hopping code modulates a sensor signal $V_{S,i}$ to one of the 8 frequency channels $f_j$, where it is superimposed with several other sensor signals. Unique connections between the hopping-code bits H[2:0] and DCO frequency-control bits X[N-1:0] allow sensor signals to combine in a different, predetermined superposition for each value of the H[2:0] sequence (i.e. 000, 001, … ,111). Thus, scanning the $2^N$ codes enables separation of all sensor signals.

Except for codes H[2:0] = 000/111, DCO connections can be designed to give a nearly uniform number of sensors in each frequency channel $f_j$. In particular, H[2:0] = 000/111 can be avoided, as $2^N$ - 2 codes provide enough information for $V_{S,i}$ separation, reducing the dynamic range required of CMOS circuitry, where a transimpedance-amplifier (TIA) output $V_{TIA}$ represents the current from all oscillators (through $C_C$). For $V_{S,i}$ separation, a relationship $\boldsymbol{y} = \mathbf{T} \cdot \boldsymbol{s}$ is formed, where $\boldsymbol{s}$ is a vector of sensor signals (derived from all $V_{S,i}$), $\boldsymbol{y}$ is a vector of the superposition in each frequency channel $f_j$ for all the hopping-code values (derived from $V_{TIA}$), and $\mathbf{T}$ is a matrix whose rows (with elements nominally 0/1) specify which $V_{S,i}$ are modulated to which $f_j$ for each hopping code. Sensor signals are separated via matrix inversion $\boldsymbol{s} = \mathbf{T}^{-1}\boldsymbol{y}$; Thus, the matrix rank achievable for $\mathbf{T}$ sets the number of sensors in Fig. 15.1.1.

This approach requires the DCOs to be phase/frequency synchronized, which is achieved by injection locking, as shown in Fig. 15.1.4. Setting the TIAs' non-inverting terminals to the sum of 8 reference sinusoids (where $V_{REF,j}$ has frequency $f_j$), the reference sinusoids appear at the virtual-ground nodes, which couple through $C_C$ to injection lock all oscillators in their respective frequency channels. Simultaneous locking of all channels is possible by setting $V_{REF,j}$ amplitudes that restrict the lock range to less than the channel separation [2]. To retrieve the total amplitude of channel $f_j$ (set by all $V_{S,i}$ at $f_j$), first the component in $V_{TIA}$ due to the reference signals is subtracted, then demodulation is performed by multiplication with the corresponding $V_{REF,j}$. For a locked DCO, the amplitude $V_{DCO,i}$ and phase $\theta_{DCO,i}$ (with respect to the reference signal, offset by $\pi/2$) depend on the value of $V_{S,i}$ as well as the difference between free-running and reference frequency $\Delta f_{LOCK,i}$ (resulting from TFT tank-capacitance variation) [2]. While the $V_{DCO,i}$ dependence on $V_{S,i}$ is desired, the $\theta_{DCO,i}$ dependence causes nonlinearity, shown next to be small. The $V_{DCO,i}$ and $\theta_{DCO,i}$ dependencies on $\Delta f_{LOCK,i}$ result only in a change of slope of the $V_{S,i}$-to-$V_{DCO,i}$ transfer function, which is easily calibrated. The simulated $V_{DCO,i}$ and $\theta_{DCO,i}$ of a locked DCO are shown in Fig. 15.1.4 for all 8 frequency channels as $\Delta f_{LOCK,i}$ is varied across the lock range (with $V_{S,i}$ fixed).

Figure 15.1.5 shows power spectral density measurements taken for 11 free-running and injection-locked DCOs for all frequency channels. The spread in free-running frequencies results from process-induced variation of the TFT capacitances $C_{TFT} = C_{GD} + C_{GS}$, which is low with respect to the channel separation (measured $\sigma(C_{TFT})/\mu(C_{TFT})$ = 0.035 across the 75mm square substrate), thus enabling successful locking in all 8 channels. Flexing can cause additional inductance variation of planar coils, though $C_{TFT}$ remains fairly constant [1]. Injection locking substantially improves the spectral purity, further enhancing the number of frequency channels possible in such a system. Representative transfer functions $O_{i,j}$ shown for a locked oscillator (from $V_{S,i}$ to demodulated-$V_{TIA}$ output, incremental with respect to $V_{S,i}$ = 10.8V) are linear over the target range (in higher $f_j$, higher tank Q and $C_C$ current cause higher slope). This linearity is critical for sensor separation via matrix $\mathbf{T}$.

The testing setup (Fig. 15.1.6) includes a large-area pressure-sensing plane with 18 piezoresistive sensors [3] in a voltage-divider configuration, a high-density probe card (including large-area inductors) for interfacing with TFT circuits, and a DAQ to acquire/drive signals for post-processing and detailed characterization. Figure 15.1.7 shows an array of ZnO-TFT DCOs. They are plastic-compatible (maximum process temperature of 180°C) but made on glass for testability with a probe card. Hopping transients are found to settle in 40µs, but a hopping rate of 240µs is employed for aggressive DSP filtering of $V_{TIA}$ following demodulation. The measured acquisition error of the system, sweeping all $V_{S,i}$ inputs over the target range (10.8V-to-11.8V), is < 0.27%. Reconstruction from sensor data for 6 different weight patterns is also shown, comparing the raw $V_{S,i}$ from sensors with variation (inset) to those acquired by the system (error shown).

*Acknowledgements:*
Funding was provided by NSF (grants ECCS-1202168, CCF-1218206), and Systems on Nanoscale Information fabriCs (SONIC), one of six SRC STARnet Centers sponsored by MARCO and DARPA. The authors thank Lung-Yen Chen for testing support.

*References:*

[1] Y. Afsar, et al., "Oxide TFT LC Oscillators on Glass and Plastic for Wireless Functions in Large-Area Flexible Electronic Systems," *SID Symp. Dig. Tech. Papers*, pp. 207-210, May 2016.

[2] B. Razavi, "A Study of Injection Locking and Pulling in Oscillators," *IEEE J. Solid-State Circuits*, vol. 39, no. 9, pp. 1415-1424, Sept. 2004.

[3] Interlink Electronics. FSR 400. [Online].
Available: http://www.interlinkelectronics.com/.

 978-1-5090-3758-2/17/$31.00 

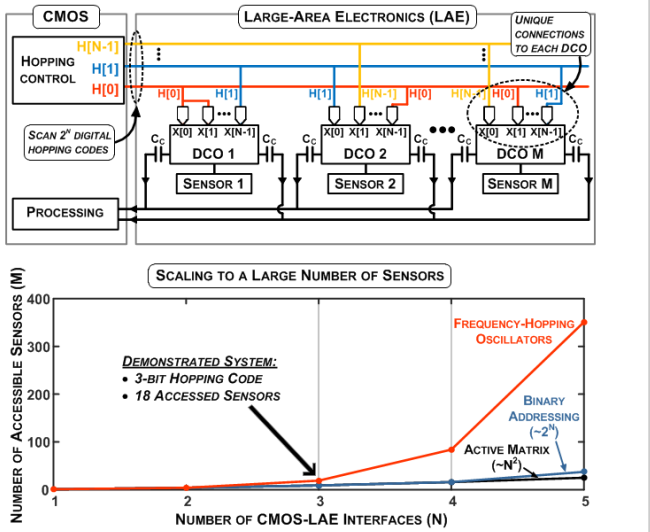


Figure 15.1.1: System architecture with sensor-modulated DCOs uniquely hardwired to CMOS enables large number of sensors (below).

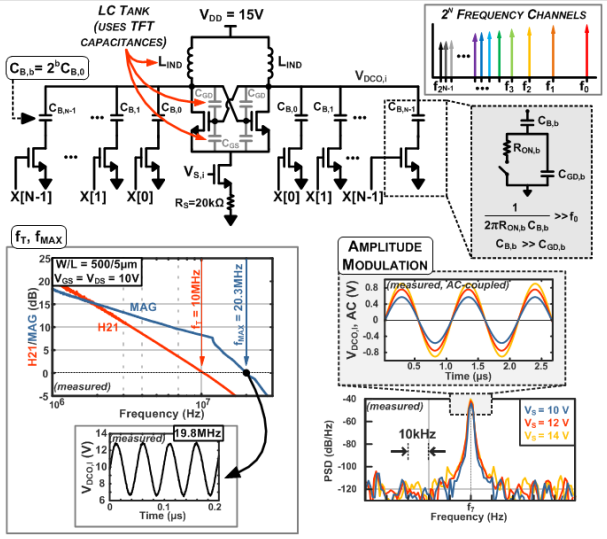


Figure 15.1.2: ZnO TFT DCO schematic. DCO amplitude modulated by sensor signal; DCO frequency modulated via switched bank capacitors.

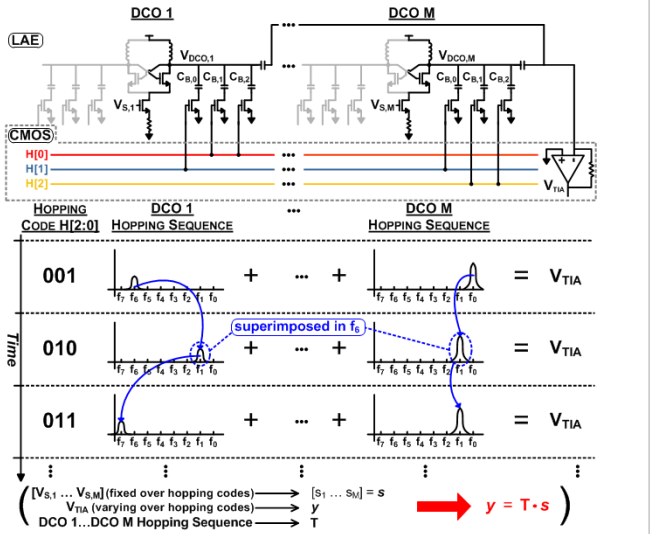


Figure 15.1.3: DCO frequency hopping causes different $V_{S,i}$ superpositions. Unique hopping sequences enable sensor separation.

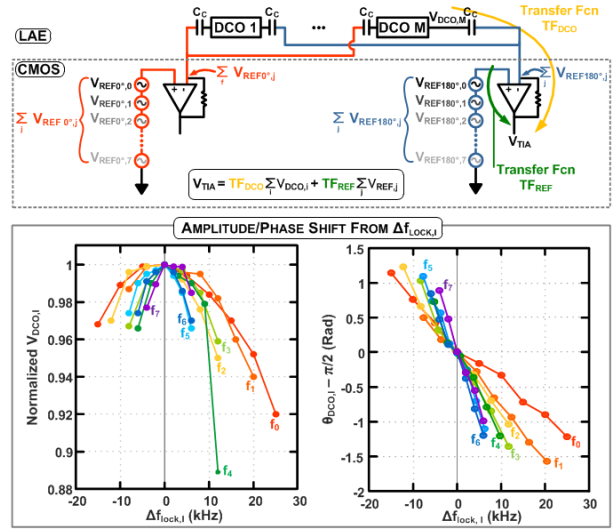


Figure 15.1.4: Injection-locking of DCOs with reference signals $V_{REF,j}$ applied to CMOS TIA. $\Delta f_{LOCK,i}$ impacts DCO amplitude and phase.

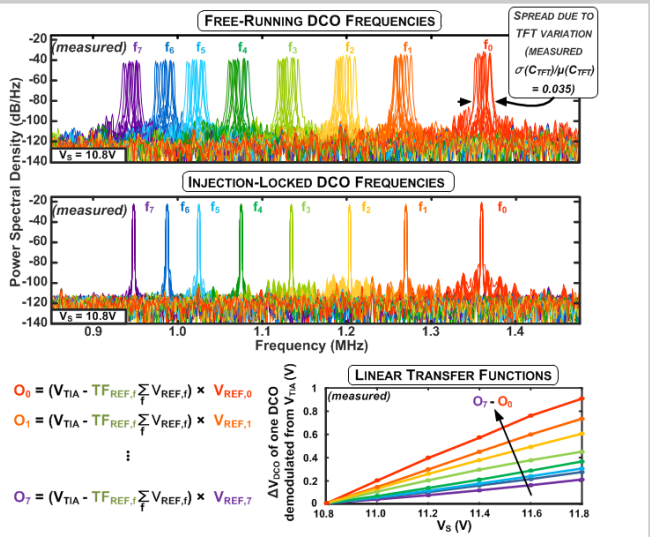


Figure 15.1.5: PSDs of free-running and injection-locked DCOs. $V_{S,i}$-to-$V_{DCO,i}$ transfer functions $O_{i,j}$ exhibit linearity over target $V_{S,i}$ range.

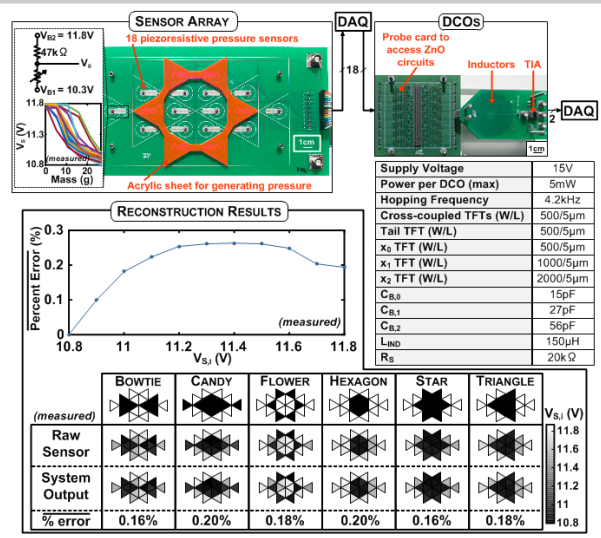


| | |
|---|---|
| Supply Voltage | 15V |
| Power per DCO (max) | 5mW |
| Hopping Frequency | 4.2kHz |
| Cross-coupled TFTs (W/L) | 500/5μm |
| Tail TFT (W/L) | 500/5μm |
| $x_0$ TFT (W/L) | 500/5μm |
| $x_1$ TFT (W/L) | 1000/5μm |
| $x_2$ TFT (W/L) | 2000/5μm |
| $C_{B,0}$ | 15pF |
| $C_{B,1}$ | 27pF |
| $C_{B,2}$ | 56pF |
| $L_{IND}$ | 150μH |
| $R_S$ | 20kΩ |

Figure 15.1.6: System testing. Setup includes pressure-sensing plane and probe card to ZnO sample, results show <0.27% acquisition error.

15

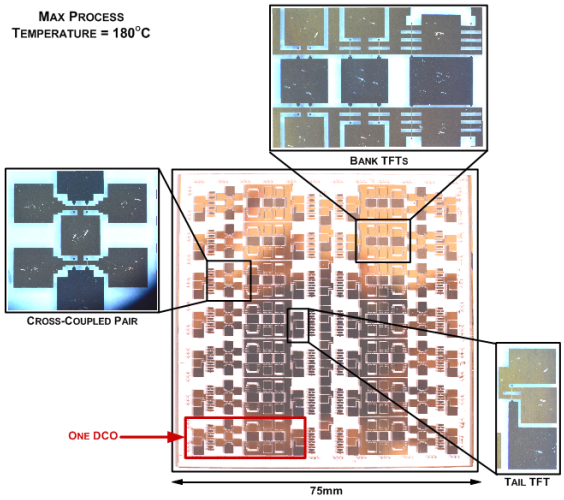


**Figure 15.1.7: Prototype 75mm×75mm sample on glass, with insets showing all ZnO TFT circuits in DCOs (fabricated at max temperature = 180°C). System measurements are taken using DCOs from two such samples.**


978-1-5090-3758-2/17/$31.00 